Molecular Weight Dependent Fragmentation of Selectively Deuterated Polystyrenes in ToF−SIMS

X. Vanden Eynde,*,†,‡ K. Reihs,‖ and P. Bertrand‡

Unité de Physico-Chimie et de Physique des Matériaux, UCL Place Croix du Sud 1, B-1348 Louvain-la-Neuve, Belgium, and Central Research-Physics, Bayer AG, Bldg E41, D-51369 Leverkusen, Germany

Received October 5, 1998; Revised Manuscript Received February 12, 1999

ABSTRACT: Two series of monodisperse polystyrenes were synthesized by an anionic polymerization initiated with *sec*-butyllithium. The number average molecular weights of the macrochains range from 1700 to 93300. The first series consist of deuterated repeat units and hydrogenated end groups (*sec*-PD_8S-H). The other one was fully hydrogenated except for one end group, which was selectively deuterated (*sec*-PS−D). The sample molecular structures are $C_4H_9(C_8D_8)_nH$ and $C_4H_9(C_8H_8)_nD$, respectively. These polymers were then analyzed by time-of-flight secondary ion mass spectrometry (ToF−SIMS). All secondary ion intensities are corrected for the carbon and deuterium isotopic distributions. Static SIMS spectra of *sec*-PD_8S-H show characteristic peaks with even masses (fully deuterated, i.e., $C_7D_7^+$, $C_6D_5^+$ at $m/z = 98, 82$) and odd peaks (containing at least one hydrogen atom, i.e., $C_7HD_6^+$, $C_6HD_4^+$ at $m/z = 97, 81$). Typically, these odd peaks show decreasing intensities as the molecular weight increases. In the *sec*-PS−D SIMS spectra, the characteristic peaks are similar to those observed for the usual polystyrene with a more specific peak at $m/z = 92$ which is related to the deuterium end group. From the molecular weight dependent intensities, it can be deduced that a hydrogen transfer occurs from the *sec*-butyl end group to the first repeat unit and promotes the formation of the tropylium fragment. A rearrangement ion formation mechanism is proposed. For both polymers, characteristic peaks of the end group are detected. With the intensity ratios of a main chain fragment and these end groups characteristic peaks, we are able to calibrate the number average molecular weight at the polymer surface. Moreover, it is shown that the main chain deuteration influences the end group segregation toward the surface.

Introduction

Static secondary ion mass spectrometry (SSIMS) allows the determination of the number average molecular weight of polymers by the emission of intact oligomers ($m/z > 1000$).[1] Their emission is obtained by the cationization of a macrochain with a substrate atomic ion when a submonolayer polymer film is deposited onto a metallic surface.[2,3] However, the characterization of bulk and surface molecular weight is of great interest for technical polymer surfaces and cannot be discovered by this method. In the literature and from our former work, it has been shown that the molecular weight of polymer chains can be determined by looking at the intensities of the characteristic end group fragments present in the fingerprint part of the SIMS spectrum (with $m/z < 250$).[4,5] A practical example has been shown by Reihs et al.[6] The spectrum calibration obtained with polycarbonates was used to image the surface spatial distribution of the polymer molecular weight in a compact disk. Nevertheless, in many cases, this M_n determination was restricted to the short chains (below 20 repeat units).

The process of secondary ion formation and emission is not yet fully understood. Recent studies have shown that matrix effects are less important for polymers analyzed in the static mode than for inorganic material analyzed in the dynamic mode but are still present.[7,8] Therefore, the fragments to be used for quantification have to be chosen with care. Weng et al. showed that, for some specific fragments, the sensitivity factors of a chemical functionality can be influenced by its neighboring functionalities.[9] To progress in this field, it is important to be able to identify the different fragmentation pathways, starting from the precursor macromolecule and leading to the formation of specific secondary ion fragments. The fragmentation of low molecular weight polymers has been chosen for this purpose. Several polymers have already been investigated such as polystyrene (PS),[4,8,10−12] poly(ethylene glycol) (PEG),[13] and poly(methyl methacrylate) (PMMA).[14] In summary, it has been shown that SSIMS is sensitive to the nature of the end groups and to their isomers. The influence of the end groups on the fragmentation pathways of the main chain is not clear. For PS oligomers, some specific interactions with the end groups were deduced from the studies on cationized deuterated PS[15,16] and from the molecular weight dependencies of fingerprint fragments of hydrogenated PS (HPS).[8] A selective deuterium labeling study was undertaken to gain deeper insights into the fragmentation schemes.

For this work, two series of selectively deuterated polystyrenes were synthesized by an anionic polymerization initiated by *sec*-butyllithium. The final molecular weights range from 1700 to 93300. The first end group for all polymers is a *sec*-butyl functionality due to the chosen initiator. The molecular structures studied are drawn in Scheme 1. The polymers are labeled *sec*-PD_8S-H or *sec*-PS−D and they exhibit a deuterated or hydrogenated repeat unit and a hydrogen or deuterium atom as the second end group, respectively.

Deuterium labeling has already been used for many different purposes in SIMS. Fundamental studies used this method for the determination of the fragmentation

* To whom correspondence should be addressed.
† E-mail: VANDENEYNDE@PCPM.UCL.AC.BE.
‡ Unité de Physico-Chimie et de Physique des Materiaux.
‖ Bayer AG.

10.1021/ma981558i CCC: $18.00
Published on Web 04/13/1999

Scheme 1. Polystyrene Molecular Structures: (a) *sec*-PD_8S-H; (b) *sec*-PS−D

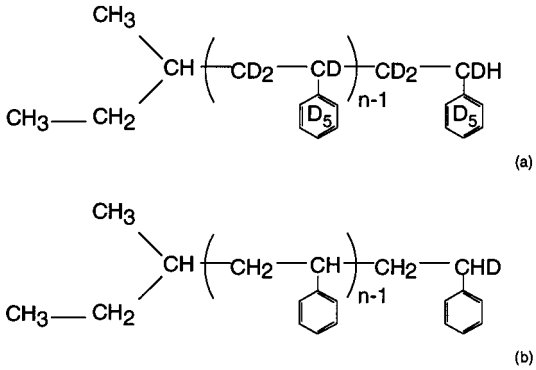

pathways by a selective deuteration of the repeat unit for PS[17−19] and PET.[20] For more practical purposes, dynamic and/or static SIMS on polymer blends containing deuterated and undeuterated macrochains allowed concentration depth profiling and surface analysis, respectively.[21−23] With these techniques, the diffusion of polymer chains through an interface or toward the uppermost surface was studied.[23−25] Other applications follow the specificity of chemical surface reactions[26] and plasma functionalizations.[27] In other cases, selective deuteration was used to overcome the poor mass resolution of quadrupole mass spectrometers in the first generation mass spectrometers used in static SIMS.

A model previously established was used to interpret the influence of the molecular weight on the SIMS intensities.[8] In this model, the absolute intensity of a fragment j, Y_j, is expressed as a sum of different contributions coming from the end groups ($Y_{E1,j}$ and $Y_{E2,j}$) and from the main chain, $Y_{M,j}$. An extra parameter (α) is used to take into account the interaction of the end group with the first adjacent repeat unit.

$$Y_j = \frac{1}{n+2}(Y_{E1,j} + Y_{E2,j}) + \frac{n-1+\alpha}{n+2}Y_{M,j} \qquad (1)$$

Here n is the average number of repeat units ($\langle n \rangle$).

The previous equation is rewritten as follows:

$$Y_j = \frac{2}{n+2}A + \frac{n}{n+2}B \qquad (2)$$

Here A and B are the end group and the main chain parameters, respectively.

On the basis of the fingerprint ions, several methods have been used to quantify the molecular weight at the surface. If some fragments appear to be only due to the main chain (Y_{MC}) and others to the end group (Y_{EG}), a univariate calibration between their intensity ratio (Y_{MC}/Y_{EG}) and the average number of repeat units ($\langle n \rangle$) may give a linear relationship used for the calibration.[4] However, for hydrogenated polystyrene (HPS), almost all ion intensities are influenced by the presence of the end groups and a similar linear calibration cannot be achieved. Indeed, for low molecular weight PS, there is no ion exclusively formed by the main chain.[8] To bypass this problem, a chemometric method, principal component analysis (PCA), was used for quantification but this method is still restricted to PS molecular weights below 10 000.[28]

Experimental Setup

Polymer Materials. The monodisperse selectively deuterated polystyrenes were purchased from Polymer Standard Services (Mainz, Germany). The *sec*-PD_8S-H samples were synthesized by anionic polymerization[29,30] of deuterated styrene units (C_8D_8 with a deuterium content compared to hydrogen of about 99%) with hydrogenated *sec*-butyllithium initiator (C_4H_9Li). The polymerization process was stopped with hydrogenated methanol (CH_3OH) in order to attach one hydrogen atom at the second end group. The two end groups of *sec*-PD_8S-H are, respectively, hydrogenated *sec*-butyl (E_1) and hydrogen (E_2). The molecular weights obtained range from 3000 to 93300. The *sec*-PS−D samples were synthesized by anionic polymerization of hydrogenated styrene units (C_8H_8) with hydrogenated *sec*-butyllithium initiator (C_4H_9Li). The polymerization was stopped by the adjunction of deuterated methanol into the reaction media (CD_3OD) in order to attach a deuterium at the second end group. Following this procedure, the two polymer end groups of *sec*-PS−D are, then, hydrogenated *sec*-butyl (E_1) and deuterium (E_2). The obtained molecular structures are drawn in Scheme 1. The obtained molecular weights range from 1700 to 22000. The number average molecular weights and polydispersity coefficients were measured by gel permeation chromatography (GPC) and they are listed in Table 1. In this work, the average number of repeat units is used in place of the molecular weight (Table 1).

Table 1. Number Average Molecular Weights and Repeat Units (M_n and $\langle n \rangle$, Respectively) and Polydispersity Coefficient (H) Measured by GPC for Deuterated Polystyrene Samples

samples	no. av molecular weight (M_n)	av no. of monomer units ($\langle n \rangle$)	polydispersity coeff (H)
PD_8S-03	3000	26	1.05
PD_8S-04	4170	37	1.04
PD_8S-05	5300	47	1.04
PD_8S-25	25100	224	1.02
PD_8S-64	64100	572	1.02
PD_8S-93	93300	833	1.01
PS−D-01	1790	16	1.07
PS−D-02	2280	21	1.06
PS−D-03	2950	28	1.05
PS−D-08	8300	79	1.04
PS−D-16	15600	149	1.04
PS−D-22	22000	211	1.02

Sample Preparation. Polymer films were prepared by solution spin coating by deposition of the polymer solution (30 mg/mL in toluene (HPLC grade solvent from Union Chimique Belge)) onto a polished single crystal silicon wafer (used as received) at 5000 rpm spinning speed and room temperature for 1 min.

ToF−SIMS Measurements. The ToF−SIMS measurements were carried out with the Charles Evans & Associates TFS-4000 MMI system using a $^{69}Ga^+$ (15 keV) liquid metal ion source. In this system, the secondary ions were accelerated up to a 3 keV energy before being 270° deflected by three electrostatic hemispherical analyzers (TRIFT).[31−33] A 800 pA DC primary ion beam was pulsed at a 5 kHz frequency with an unbunched pulse width of 23 ns and is rastered over a 130 × 130 μm^2 surface area. All spectra were acquired for 10 min with a fluence ~ 10^{12} ions/cm^2 ensuring static conditions. A mass resolution m/Δm of ~ 6000 measured at $m/z = 28$ on a Si wafer was achieved. No charge compensation was needed for spin coated films, in this study. As the negative SIMS spectra of PS contain much less information on the polymer molecular structure than the positive ones, they are not discussed in this paper.

All films seemed free of cracks or defects, as checked by the absence of the silicon substrate signal (Si^+, at $m/z = 28$) in the spectra. These samples did not contain any additives. The contaminants for spin-coated films were mainly alkali or halogens (i.e. Li^+, Na^+, or Cl^- at $m/z = 7$, 23, and 35/37, respectively). Li^+ at $m/z = 6$ and 7 remains from the polymerization process. The reproducibility of the absolute intensities was estimated from the variance obtained for at least four independent measurements. The standard deviation was found to be ~10% of the mean normalized intensity value.

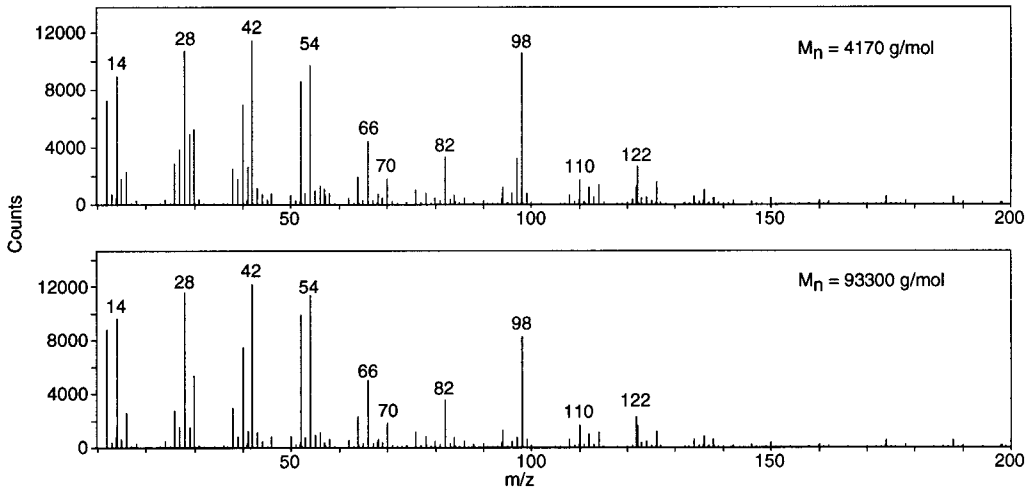

Figure 1. SIMS spectra (*m*/*z* from 5 to 200) of monodisperse *sec*-PD_8S-H: M_n = 4170 (top) and 93300 (bottom).

Data Treatment. The first data treatment of the raw spectra was performed with Cadence 1 software from Charles Evans & Associates. For each spectrum *i* (e.g. Figure 1), all secondary ion (SI) peak intensities corresponding to the different ion structures *j* were measured and quoted as $Y_{i,j}$. As most as possible, the intensities due to unimolecular dissociation were not involved into our data. Indeed, if unimolecular dissociation occurs, the ionized daughter ions are observed as new peaks and then this is easy to separate the additional contributions.[34]

Since the high mass resolution is, up to now, insufficient to discriminate ^{13}C containing ions from the ^{12}C ones, isotopic corrections have to be performed on all the absolute intensities in order to take into account the natural isotopic distribution (NID) of the carbon atom. Carbon has two isotopes at *m*/*z* = 12 and 13 with the natural isotopic ratios of 98.9% and 1.1%, respectively. For a ^{13}C correction, the absolute intensity Y_j at $m/z = j$ is multiplied by 1.011*x* to obtain the corrected intensity Y_j*, and the absolute intensity Y_{j+1} at $m/z = j + 1$ is reduced by $(0.011x)Y_j$ in order to remove the $^{13}CC_{x-1}H_y$ contribution at $m/z = j + 1$, leaving only the C_xH_{y+1} one. Another isotopic correction had to be performed due to the incomplete deuteration of the styrene repeat units, which was about 99% D. If a fragment C_xD_y is produced, another fragment can be produced with exactly the same molecular structure and precursor but with one deuterium replaced by one hydrogen (C_xHD_{y-1}). The intensity of C_xHD_{y-1} is then partly caused by the uncompleted deuteration of C_xD_y. The correction consisted in the subtraction of $y(1 - d)C_xD_y$ intensity (at $m/z = j$) from the C_xHD_{y-1} intensity (at $m/z = j - 1$). For the *sec*-PS−D data, we assume that the deuterium attachment yield at the end group is 100%. After these corrections, the absolute intensities are free of any isotopic contributions.

Moreover, the normalization is needed in order to eliminate the systematic differences in the absolute intensities measured on replicate spectra. These differences between replicate spectra might be due to slight differences in the experimental settings. Then before comparing different sets of samples, the normalization of the different experiments was performed by the extrapolated intensity at high molecular weight.[8] This last value was obtained by fitting the data with the model presented in ref 8.

$$N_{j,n} = \frac{Y_{j,n}}{\lim_{n\to\infty} Y_{j,n}} \qquad (3)$$

Here $N_{j,n}$ is the normalized intensity and $Y_{j,n}$ is the absolute intensity at molecular weight equal to *n* for the fragment *j*.

Results

The hydrogenated polystyrene (HPS) SIMS spectrum had already been reported in the literature.[35−37] It is characterized by a series of unsaturated and aromatic fragment ions (at *m*/*z* = 26, 39, 51, 63, 77, 91, 103, 105, 115, 128, 141, 152, and 165 ...). The deuterated polystyrene SIMS spectra are presented in Figure 1 for M_n = 4170 and 93300. The SIMS fingerprint of *sec*-PD_8S-H is quite different from the HPS one. Most of the characteristic fragments have the same molecular structure as in the HPS SIMS spectrum but with their hydrogen atoms replaced by deuterium atoms. Indeed, the HPS fragments with $C_xH_y^+$ molecular structures (at $m/z = j$) are shifted to $C_xD_y^+$ (at $m/z = j + y$) in the *sec*-PD_8S-H spectrum. For instance, the peak at *m*/*z* = 77, $C_6H_5^+$, in HPS spectrum corresponds, for the deuterated PS to $C_6D_5^+$ at *m*/*z* = 82 and similarly, for $C_7D_7^+$, $C_8D_7^+$, $C_8D_9^+$, and $C_9D_7^+$ at *m*/*z* = 98, 110, 114, and 122, respectively. All the odd peaks contain at least one hydrogen atom within their molecular structure, such as $C_7HD_6^+$ at *m*/*z* = 97. The *sec*-butyl end group has the same parent ion ($C_4H_9^+$ at *m*/*z* = 57). It is seen in the spectra that the intensities at *m*/*z* = 57 and 97 decrease when the molecular weight is increased. In contrast, the peak at *m*/*z* = 98 remains almost unchanged.

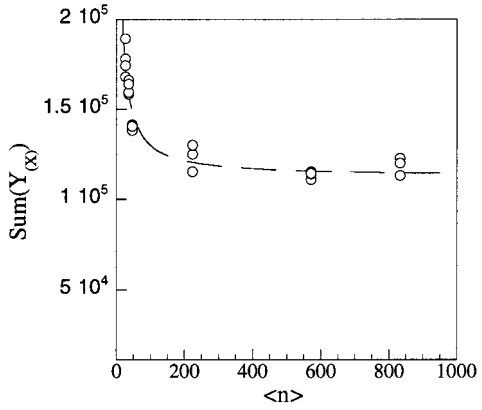

Figure 2. Total intensity I^b_{total} of *sec*-PD_8S-H vs the average number of repeat units ($\langle n \rangle$).

The total intensity in *sec*-PD_8S-H SIMS spectra is plotted in Figure 2 as a function of the average number of repeat units ($\langle n \rangle$). An increase at low $\langle n \rangle$ is observed. A similar effect has been reported for *sec*-PS−H.[8,12] This increase suggests that specific fragmentation mechanisms are significant at low molecular weight. It shows that polymer end groups play an important role on the secondary ion formation when their concentrations are

Table 2. Different Types of Ions in the DPS Spectra as a Function of the Molecular Weight

cluster *x*	$C_xD_y^+$ (DI) (*m*/*z*)	$C_xD_y^+$ (DII) (*m*/*z*)	$C_xHD_{y-1}^+$ (HI) (*m*/*z*)
1	14, 16, 18	-	13, 15, 17
2	24, 28, 34	26, 30	25, 27, 29, 33
3	36, 38, 40, 42	44, 46	37, 39, 41, 43, 45
4	50, 52, 54	56, 58, 60	51, 53, 55, 57, 59, 61
5	62, 64, 66, 68	70, 72	63, 65, 67, 69, 71, 73
6	74, 76, 78, 80, 82, 84	86	77, 79, 81, 83, 85
7	88, 90, 92, 94,	96, 98, 100	89, 91, 93, 95, 97, 99, 101
8	104, 106, 108	110, 112, 114, 116	107, 109, 111, 113, 115
9		118, 120, 122, 124, 126, 128	119, 121, 123, 125, 127
10		132, 134, 136, 138, 140, 142	133, 135, 137, 139, 141, 143

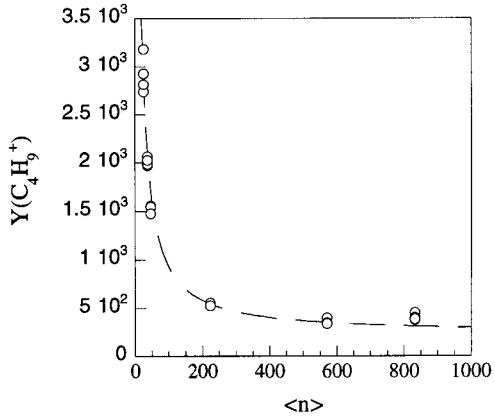

Figure 3. *Sec*-butyl end group parent ion, $C_4H_9^+$, absolute intensity ($Y_{(57)}$) in *sec*-PD_8S-H vs $\langle n \rangle$.

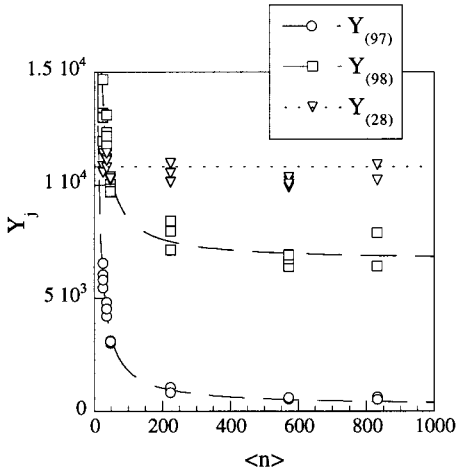

Figure 4. $Y_{(28)}$, $Y_{(97)}$, and $Y_{(98)}$ vs $\langle n \rangle$ for *sec*-PD_8S-H. Peaks at $m/z = 28$, 98, and 97 are defined as types DI, DII, and HI, respectively (see text).

high, at low molecular weight. Indeed, the end group parent ($C_4H_9^+$ at $m/z = 57$) ion intensity increases also with the decrease of $\langle n \rangle$ (Figure 3). However, it is observed that fragment at $m/z = 28$ is not influenced by the increase of M_n, whereas that at $m/z = 98$ is slightly influenced and that at $m/z = 97$ decreases strongly. Moreover, as in the HPS spectrum,[8] most of the characteristic *sec*-PD_8S-H peaks vary with the amount of the *sec*-butyl end groups and then, obviously, with the molecular weight. In the *sec*-PD_8S-H spectra, three types of fragments can be determined owing to their molecular weight dependent behavior. The even peaks ($C_xD_y^+$) show two different behaviors. The first type of peaks (DI) exhibits an absolute intensity remaining almost constant over the entire range of molecular weight. The second type (DII) exhibits a slight increase of the absolute intensity for the low molecular weight samples as shown in Figure 4 for $C_7D_7^+$ at $m/z = 98$. By contrast, the odd mass peaks ($C_xHD_{y-1}^+$) exhibit a large increase of their absolute intensity at low molecular weight as shown in Figure 4 for $C_7HD_6^+$ at $m/z = 97$ and correspond to the HI type. Table 2 summarizes, for each cluster, the different types of ions present in the *sec*-PD_8S-H SIMS spectra. For the clusters with less than six carbon atoms, the *sec*-PD_8S-H characteristic peaks ($C_2D_2^+$, $C_3D_3^+$, $C_4D_3^+$, $C_5D_3^+$, $C_6D_3^+$, and $C_6D_5^+$ at $m/z = 28$, 42, 54, 66, 78, and 82, respectively) are unchanged with the molecular weight (ions of DI type). Therefore, their formation is independent of the end groups. The various mechanisms leading to their production were already discussed by several authors.[17−19,38−40] For the clusters containing more than six carbon atoms, the *sec*-PD_8S-H characteristic peaks ($C_7D_7^+$, $C_8D_7^+$, $C_8D_9^+$, and $C_9D_7^+$ at $m/z = 98$, 110, 114, and 122, respectively) are ions of DII type with their intensities slightly increasing for the low molecular weights.

The *sec*-PS−D SIMS spectra of a low and a high molecular weight sample are displayed in Figure 5. They look very similar to the spectra for *sec*-PS−H. Indeed, the characteristic peaks appear at the same mass: $m/z = 26$, 39, 53, 63, 77, 91, 103, 105, 128, 141, 152, and 165 .... Their exact molecular structures are much more difficult to define exactly due to the presence of the D isotopic labeling at one end group. For the high molecular weight spectra, this effect can at first be neglected and the fragment molecular structures are similar to those observed for HPS and *sec*-PS−H. A peak at $m/z = 57$ is also observed in the SIMS spectra that is also related to the *sec*-butyl end group parent ion ($C_4H_9^+$). This peak exhibits a higher intensity for the low molecular weight samples. The absolute intensity of the fragment at $m/z = 91$, just like the relative intensity compared to the peak at $m/z = 92$, increases for low molecular weight polystyrenes (Figure 5).

The total intensity of the SIMS *sec*-PS−D spectra is also seen to decrease when M_n increases similarly to previous *sec*-PD_8S-H results. This increase is due to a specific fragmentation induced by the large presence of the end groups at low molecular weights. Indeed, the butyl parent ion intensity at $m/z = 57$ increases at low $\langle n \rangle$ and follows the same behavior than in SIMS *sec*-PD_8S-H spectra. The most intense peak in these SIMS spectra is associated with $C_7H_7^+$ or tropylium ion at $m/z = 91$. In Figure 6, the absolute intensity of $C_7H_7^+$ is plotted as a function of $\langle n \rangle$. Its intensity decreases when increasing $\langle n \rangle$. Similarly, the peak at $m/z = 92$ exhibits an intensity decrease for the high molecular weight samples. Usually, in SIMS PS spectrum, the peak at $m/z = 92$ is due to the natural isotopic distribution of the carbon atoms present in the $C_7H_7^+$ fragment. But, compared to that at $m/z = 91$, this peak exhibits an

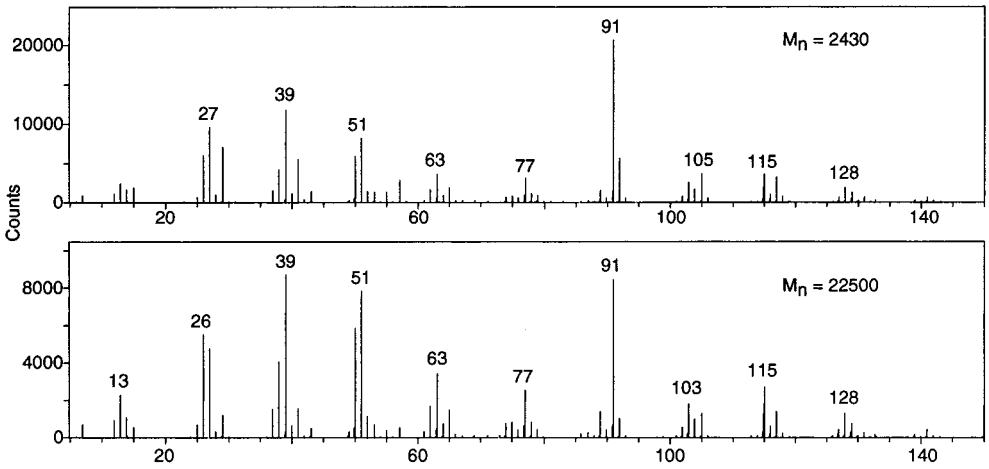

Figure 5. SIMS spectra (*m*/*z* from 5 to 150) of monodisperse *sec*-PS−D: M_n = 2430 (top) and 22500 (bottom).

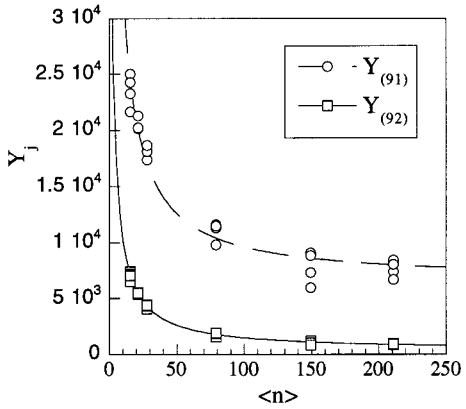

Figure 6. Tropylium absolute intensities, $Y_{(91)}$ and $Y_{(92)}$ in *sec*-PS−D vs ⟨*n*⟩.

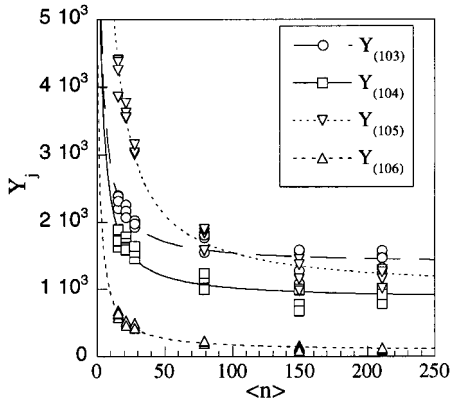

Figure 7. Absolute intensities of $Y_{(103)}$, $Y_{(104)}$, $Y_{(105)}$, and $Y_{(106)}$ in *sec*-PS−D vs ⟨*n*⟩.

additional intensity believed to be due the deuterium end group and associated to the $C_7H_6D^+$ molecular ion. In Figure 7, the peak intensities at *m*/*z* = 103, 104, 105, and 106 for *sec*-PS−D are displayed as a function of the number of repeat units, ⟨*n*⟩. As a general observation, their intensities decrease when ⟨*n*⟩ is increased. Moreover, this decrease is stronger for the fragments with high hydrogen content.

Discussion

The following discussion is divided in three parts. In the first part, the molecular weight dependent intensities of the characteristic PS secondary ions are discussed for both series of deuterated samples and compared to previous data obtained with hydrogenated polystyrenes, *sec*-PS−H.[8] In the second part, it will be shown that the selective deuteration of the main chain induces a reorientation of the end groups at the surface. In the last part, a specific fragmentation pathway for the polystyrene chains, namely the H transfer, is proposed to interpret the molecular weight effects. This fragmentation scheme is generalized for a possible main chain rearrangement leading to the formation of PS characteristic secondary ions.

(1) Molecular Weight Dependent Intensities. The end group parent ion ($C_4H_9^+$) is present in *sec*-PD_8S−H and *sec*-PS−D SIMS spectra at *m*/*z* = 57. This ion exhibits a decrease of its intensity for high molecular weight (Figure 3) as for *sec*-PS−H samples (see Figure 4 in ref 8). But its intensity does not vanish at high M_n, and it exhibits a saturation value that is observed for all the samples. This is explained either by an alkyl contamination, or its formation comes from either the styrene units, or from the end group. Since the $C_4D_9^+$ ion is absent in the *sec*-PD_8S−H spectrum, the butyl fragments are not produced by a main chain rearrangement whatever the M_n. An end-group peak intensity should approach zero at infinite macromolecule length; thus, the remaining part of the intensity at high molecular weight cannot come from the end group. This contribution is believed to be due to a residual hydrocarbon contamination.

Before the absolute intensities observed in the *sec*-PD_8S−H SIMS spectra are interpreted, they have to be corrected for the carbon NID and for the uncompleted deuteration of the styrene repeat unit (as described above). In Figure 8, the corrected intensity of *m*/*z* = 97, $Y_{(97)}$*, is plotted as a function of the average number of repeat units (⟨*n*⟩). The saturation value observed for $Y_{(97)}$ at high ⟨*n*⟩ (Figure 4) disappears after corrections and the corrected intensity approaches zero for an infinite molecular weight. The appearance of this saturation value was due to the uncompleted deuteration of the styrene repeat unit and the tropylium fragment formed within the main chain can have two equivalent molecular structures, $C_7D_7^+$ and $C_7HD_6^+$. The corrected peak intensity, $Y_{(97)}$*, can be fitted with our molecular weight model[8] (full line in Figure 8) and is proportional to 1/(*n* + 2). This shows that the peak at *m*/*z* = 97 could, after corrections, be interpreted as a characteristic end group fragment.

For *sec*-PS−D, similarly to *sec*-PD_8S−H, the isotopic corrections have to be performed. In Figure 9, the

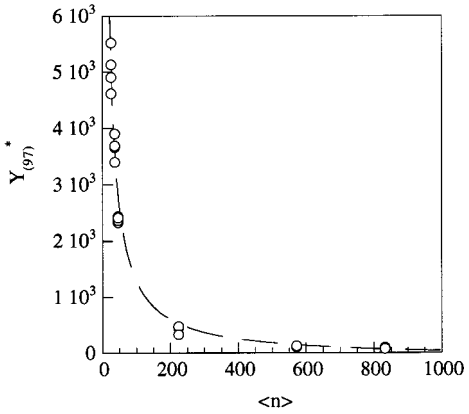

Figure 8. $Y_{(97)}$ after the isotopic corrections, $Y_{(97)}$*, vs $\langle n \rangle$ for *sec*-PD_8S−H.

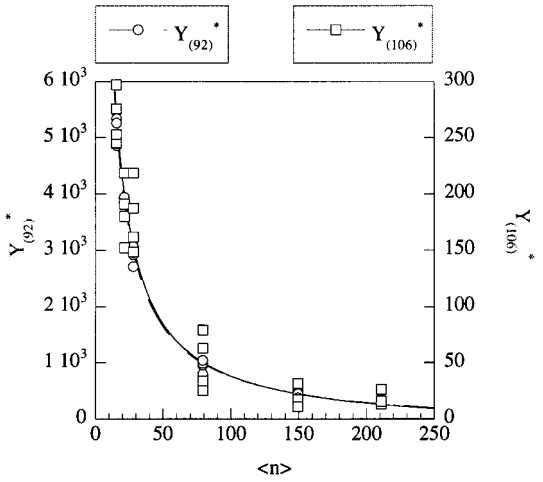

Figure 9. Absolute intensities at $m/z = 92$ and 106 after the isotopic corrections, $Y_{(92)}$* and $Y_{(106)}$*, respectively, vs $\langle n \rangle$ for *sec*-PS−D.

corrected intensity of the peak at $m/z = 92$, $Y_{(92)}$*, is plotted as a function of $\langle n \rangle$. Indeed, the carbon NID of the tropylium ion has an influence on the peak intensity at $m/z = 92$ due the $^{13}CC_6H_7^+$ molecular fragment. After the correction (see experimental part), the $Y_{(92)}$* intensity is still significant, especially at low $\langle n \rangle$. This means that there exists another fragment than $^{13}CC_6H_7^+$. This other molecular structure is related to the deuterium end group which can produce $C_7H_6D^+$ secondary ion at $m/z = 92$. Its corrected peak intensity ($Y_{(92)}$*) approaches zero for an infinite M_n and varies as $1/(n + 2)$, in agreement with our model.[8] Then, this molecular fragment is exclusively characteristic of the deuterium end group. Similarly, the corrected intensity at $m/z = 106$ is displayed in Figure 9. When compared with the uncorrected $Y_{(106)}$ intensity (Figure 9), it is easily seen that part of the $m/z = 106$ absolute intensity is due, on one hand, to the natural isotopic distribution of carbon in the $C_8H_9^+$ fragment and on the other hand, to the deuterium end group contribution. Thus the two molecular structures interfering with this peak are $^{13}CC_7H_9^+$ and $C_8H_8D^+$.

To compare the *sec*-PS−H,[6] *sec*-PD_8S−H, and the *sec*-PS−D data, the peak intensities were normalized to the extrapolated peak intensity for an infinite molecular weight, see eq 3. The comparison was performed for the fragments that are influenced by the presence of the end groups such as peaks at $m/z = 91$, 92, 97, 98, 105, and 106. Between *sec*-PS−H and *sec*-PS−D, the difference is only the second end group −H or −D, respectively. The influence of this second end group is mainly observed at $m/z = 92$. Figure 10 presents the sum of the peaks at $m/z = 91$ and 92 normalized as explained by eq 3 as a function of the number of repeat units ($\langle n \rangle$). The $A/B_{(j)}$ parameters for the peaks at $m/z = 91$, and 92 and their sum are listed in Table 3. For both end groups, −H or −D, the sum of 91 and 92 exhibits a similar $A/B_{(j)}$ ratio confirming the same end group dependence. The $A/B_{(j)}$ ratio for the sum of several peaks can be modeled as follows according to the equations detailed in ref 8:

$$\frac{A}{B}\left(\sum_{j=1}^{k} Y_j\right) = \frac{\sum_{j=1}^{k} A_j}{\sum_{j=1}^{k} B_j} \qquad (4)$$

Here A_j and B_j are the end group and the main chain parameters for the fragment j, respectively (eq 2).

In the *sec*-PS−H case, the three A/B values for $Y_{(91)}$, $Y_{(92)}$, and $Y_{(91)}+Y_{(92)}$ are very close. Then it can be assumed that these fragments have very similar fragmentation pathways and that $Y_{(92)}$ is due to the natural isotopic distribution of $C_7H_7^+$. On the contrary, the $A/B_{(j)}$ parameters for the *sec*-PS−D samples are very different. The $A/B_{(92)}$ ratio is very high whereas at $m/z = 91$ it is lower than the one observed for *sec*-PS−H. The high value of the $A/B_{(92)}$ ratio for *sec*-PS−D is due to the fact that, for PS−D, this peak is more characteristic of the deuterium end group with the $C_7H_6D^+$ composition than the main chain with the $^{13}C^{12}C_6H_7^+$ one. Nevertheless, the $A/B_{(91)}$ ratio remains significant for the *sec*-PS−D

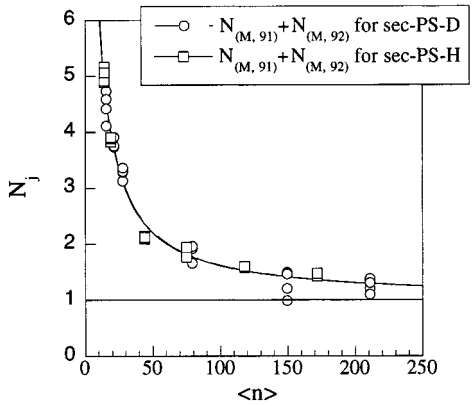

Figure 10. $N_{(91)} + N_{(92)}$ vs $\langle n \rangle$ for *sec*-PS−H and *sec*-PS−D.

Table 3. $A/B_{(j)}$ Ratios of Different Fragments at $m/z = 91$ and 92 and at 105 and 106, and Their Sums for Two Series of Polystyrenes PS−D and PS−H

	$A/B_{(j)}$	
X	*sec*-PS−H	*sec*-PS−D
91	64.4	50.3
92	66.2	370.3
91 + 92	64.6	65.3
101	6.6	7.1
102	9.7	10.1
103	12.3	13.4
104	22.3	23.6
105	69.7	65.1
106	71.6	141.2
105 + 106	70.2	70.5

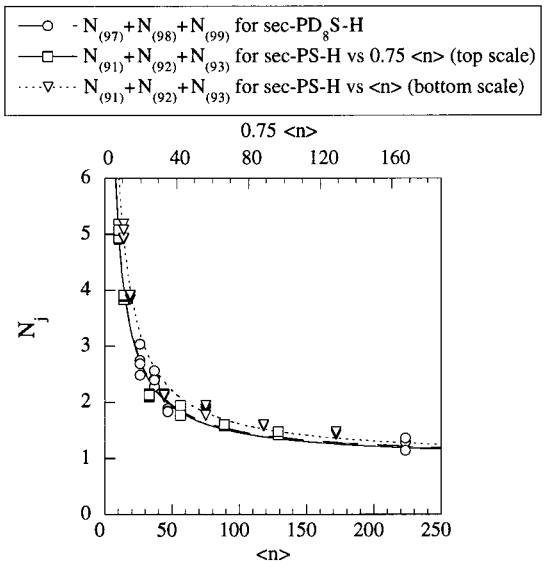

Figure 11. $N_{(91)} + N_{(92)} + N_{(93)}$ from *sec*-PS−H, $N_{(97)} + N_{(98)} + N_{(99)}$ from *sec*-PD_8S−H vs $\langle n \rangle$ and $N_{(91)} + N_{(92)} + N_{(93)}$ from *sec*-PS−H vs $S\langle n \rangle$ with $S = 0.75$ (top scale).

polymers, meaning that the other end group, namely the *sec*-butyl one, has an influence on the $C_7H_7^+$ formation. As for the tropylium fragments, the $A/B_{(105+106)}$ values (Table 3) are very close for both polymers and also close to the $A/B_{(105)}$ and $A/B_{(106)}$ values observed for *sec*-PS−H. These $A/B_{(105)}$ and $A/B_{(106)}$ values for *sec*-PS−D are lower and higher than the $A/B_{(105+106)}$ one, respectively. It seems obvious that peak at $m/z = 106$ is also directly influenced by the deuterium end group but less than peak at $m/z = 92$. By contrast, $A/B_{(j)}$ for the other peaks in the C_8 cluster (at $m/z = 101$, 102, 103, and 104) are not influenced by the replacement of the hydrogen by a deuterium end group (Table 3). Unfortunately, the $A/B_{(57)}$ ratio of parent end group ion ($C_4H_9^+$) cannot be used in the *sec*-PS−H/*sec*-PS−D comparison because, as was said before, the intensity at high M_n is only due to a hydrocarbon contamination on which there is no control.

(2) Surface Segregation. In the previous paragraph, it has been shown that, for *sec*-PS−H and *sec*-PS−D polymer, $N_{(91)} + N_{(92)}$ exhibits the same molecular weight dependence (Figure 10). Therefore, the −D end group does not segregate preferentially toward the surface as compared to the −H one. Then the too slight difference between −H and −D end groups of the *sec*-PS−H and *sec*-PS−D samples, respectively, is not sufficient to promote the segregation of this −D end group.[38,39]

In Figure 11, the sum of all the normalized intensities contributing to the tropylium structure is plotted for each type of samples as a function of the average number of repeat units ($\langle n \rangle$). These sums correspond to the normalized peak intensities at $m/z = 91$, 92, and 93, in *sec*-PS−H and *sec*-PS−D SIMS spectra, and at $m/z = 97$, 98, and 99, in *sec*-PD_8S−H. Both sums increase for the low $\langle n \rangle$, but these two molecular weight dependencies do not follow exactly the same tendencies. The *sec*-PD_8S−H series exhibits lower normalized intensities than the *sec*-PS−H one. It has been shown that the end group present at the surface can have a direct influence on the tropylium formation in SIMS. The value of the *A* parameter in eq 2 is related to the number of end groups, and then it can be used to look at the end group segregation toward the surface. Indeed, if such segregation occurs, for a given molecular weight, the end group signal will be increased.

The two curves can be superposed, if we plot $N_{(91)} + N_{(92)} + N_{(93)}$ as a function of $S\langle n \rangle$ where $S < 1$ is an adjustable parameter. The best fit (also shown in Figure 11) is obtained for $S = 0.75$. This indicates that the number of end group at the surface compared to the main chain is lower in the case of *sec*-PD_8S−H than *sec*-PS−H and *sec*-PS−D. Indeed, when the hydrogenated styrene units are replaced by deuterated ones, the average number of end groups sampled by the SIMS technique for a given molecular weight decreases by about 20−25%.

Because the C−D bonds contributes to make the surface energy lower than for C−H ones,[38] the H end groups are expected to be more oriented toward the bulk for *sec*-PD_8S−H than for *sec*-PS−H and *sec*-PS−D. The difference of surface free energy between an hydrogenous and a deuterious polystyrene has been calculated to be 0.08 mJ/m^2.[40] Indeed, the main chain deuteration in *sec*-PD_8S−H seems to decrease the number of butyl end group at the surface and then, the hydrogenated end groups seems to be less present at the surface than for *sec*-PS−H and *sec*-PS−D. This preferential surface segregation of the deuterated moieties was already observed in SIMS in a previous work with block polystyrene, P(H_8S-*b*-D_8S).[19] However, a segregation of the −D end groups at the *sec*-PS−D surface is not observed within the limit of the technique.

(3) Proposed Polystyrene Fragmentation Pathways. In the following paragraphs, the molecular weight dependent mechanisms of fragmentation are discussed in a general way for the *sec*-PS−H polymers. Two separate pathways are thought to take place: direct scission and the rearrangement before or during secondary ion emission. Due to the collision cascade from the primary ion impact, all the species around the impact region are excited. Several fragmentation pathways can follow this excitation. The first mechanism is the direct scission of the polymer bonds. This explains the formation of the parent end group ions such as $C_4H_9^+$, at $m/z = 57$, characteristic of the butyl end group for all studied polystyrenes, $C_7H_6D^+$ at $m/z = 92$ in *sec*-PS−D, and $C_7D_6H^+$ at $m/z = 97$ in *sec*-PD_8S−H (Scheme 2).

This second mechanism could be a rearrangement of the *sec*-butyl end group and the first adjacent repeat unit leading to specific ion formation. Two possible mechanisms are proposed. The first one is the McLafferty rearrangement[4,41] and the second is the 1,2 hydrogen shift.[8] Up to now, there has been no proof to distinguish between them. As a first step, the initiation of these molecular rearrangements assumes the ionization of the phenyl ring. This occurs by the release of one electron due to the energy dissipation of the primary impact in the collision cascade.[42] Then, the first mechanism (MacLafferty rearrangement) is favored through a six-membered ring transition state combining the *sec*-butyl and the first adjacent repeat unit that is promoted by the lability of a butyl hydrogen atom (Scheme 3). The hydrogen atom at the first carbon atom (γ) is transferred from the end group to the phenyl ring (γ-H rearrangement). This is followed by the scission of the $C_\alpha-C_{\beta 1}$ bond of the first adjacent repeat unit (β-cleavage), and finally, a pentene molecule is released. This mechanism is in good agreement with our previous results about the influence of the different isomer of the butyl end

Scheme 2. Fragmentation of the −D End Group and Subsequent Dehydrogenation

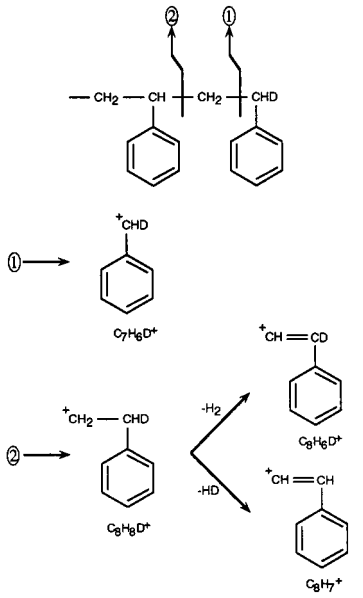

Scheme 3. Proposed Rearrangement Mechanism at the *sec*-Butyl End Group and Subsequent Fragmentations

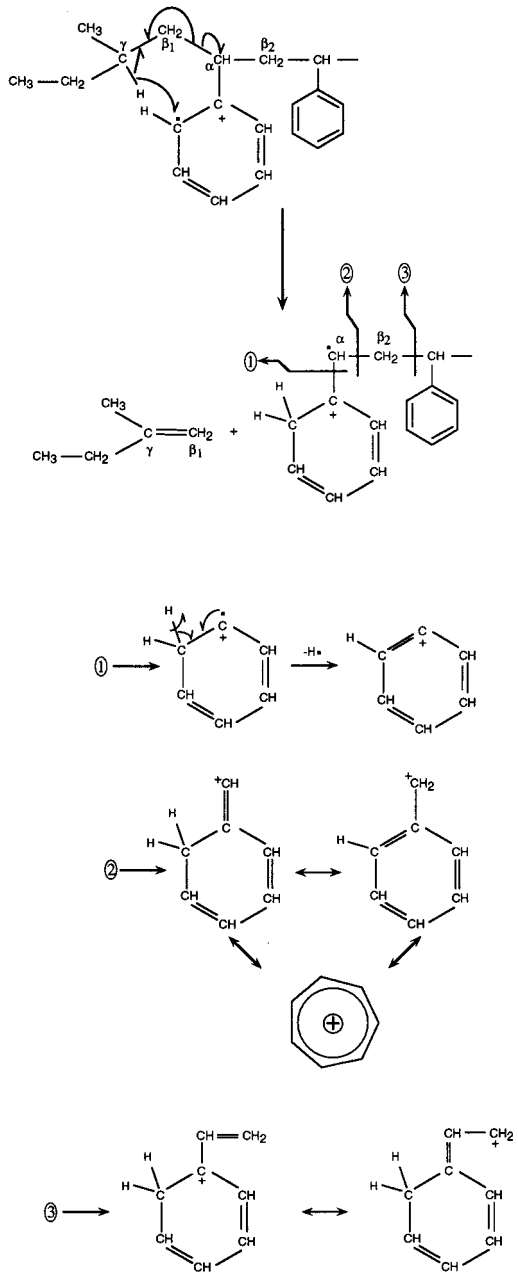

group.[8] Indeed for the *tert*-butyl, no major H transfer was observed in SIMS because the γ carbon atom is completely substituted and then, the absence of the labile H atom does not permit the rearrangement.[8] Moreover, classic mass spectrometry literature showed that this rearrangement does not occur if the ortho positions of the phenyl ring or the γ carbon atoms are completely substituted.[43] This mechanism is proposed to explain the formation of DII and HI ions observed in *sec*-PD_8S-H SIMS spectra. Indeed most of the odd peaks (HI) present in the *sec*-PD_8S-H SIMS spectra can be explained through this rearrangement mechanism (Scheme 3). For example, the $C_7HD_6^+$ at $m/z = 97$ can be formed after the H transfer toward the deuterated phenyl ring followed by the scission of a $C_\alpha-C_{\beta 2}$ bond (Scheme 3). If, in SIMS, the fragments have enough internal energy, the tropylium molecular structure (charged seven carbon atom ring) will be favored because it exhibits an energy of formation lower than other structures such as, e.g., the benzyl ion (charged phenyl−methylene).[44] This induces a scrambling of the hydrogen (or deuterium) atoms around the seven carbon atom ring as observed by Chilkoti et al. on selectively deuterated PS.[17] With this first H transfer, a similar pathway is deduced for the formation of $C_8H_9^+$ at $m/z = 105$ in *sec*-PS−H or $C_8HD_8^+$ at $m/z = 113$ in *sec*-PD_8S-H (Scheme 3). After their formation, these ions can, depending of their molecular structure and internal energy, suffer an unimolecular dissociation especially with loss of H, H_2 or loss of C_2H_2.[34,45−46] In *sec*-PD_8S-H, a subsequent dehydrogenation of these H transferred ions leads to either $C_7D_5^+$ or $C_7HD_4^+$ (at $m/z = 94$ and 93, respectively), and $C_8D_7^+$ or $C_8HD_6^+$ (at $m/z = 110$ and 109, respectively). These secondary reactions would be favored for the fragments with enough internal energy. These reactions could also be the reason for the increasing intensity of the DII ions. A similar dehydrogenation would lead, for the *sec*-PS−H polymers, to the formation of $C_7H_5^+$ and $C_8H_7^+$ at $m/z = 89$ and 103, respectively.

In this last section, a possible mechanism of H transfer is proposed for the end group interaction; however, the tropylium formation within the main chain is still unknown. The tropylium is mainly formed from the interaction of the phenyl ring with the backbone.[17] Moreover, this fragment is not produced by the subsequent fragmentation of higher mass fragments as shown by the tandem measurements.[45,46] From Chilkoti's results, it is known that, in the $C_7H_7^+$ fragment, two hydrogen atoms come from the backbone.[17] The first one is the H atom attached to the α carbon and the second one should come from somewhere else in the chain. Other results from Affrossmann, on random and block copolymers with deuterated and undeuterated styrene repeat units, showed that this interaction occurs mainly between neighboring repeat units.[18,19] Moreover, with use of the Huan et al. work on substituted polyacetylenes, a phenyl−phenyl interaction can be excluded as a pathway for the formation of a $C_7H_7^+$ ion.[47] It can be also deduced from these results that some H atoms from the backbone are needed to form the tropylium ion. Then, by analogy with the proposed H transfer mechanism detailed in the previous paragraph, we think that

Scheme 4. Proposed Rearrangement Mechanism within the Main Chain

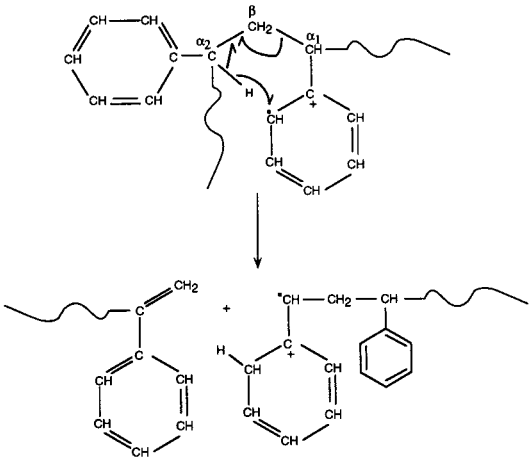

the six-membered ring rearrangement could be rewritten within the main chain by involving two adjacent repeat units in the mechanism (Scheme 4). The products of the fragmentation are a radical ionic and a neutral unsaturated end group. This unsaturated end group on large PS fragments was already observed as a major product of the ion beam interaction in SIMS analysis.[48] The radical ionic part remains active and can lead to the formation of $C_7H_7^+$ or $C_8H_9^+$ at $m/z = 91$ and 105 (as shown in Scheme 3). However, the above mechanism is one probable event among other competitive fragmentation pathways that could also take place.[12] More investigations are needed to point out all these processes.

Conclusion

Selectively deuterated polystyrenes with H- and *sec*-butyl end groups have been analyzed by time-of-flight secondary ion mass spectrometry (ToF−SIMS). The usefulness of the selectively deuterated molecular structure has been demonstrated to obtain some new insights in the fragmentation schemes for the secondary ion formation. Indeed the influence of each end group on the polystyrene fragmentation has been enlightened. Specific mechanisms of ion formation have been proposed for each end group. An H transfer between a *sec*-butyl end group and the first adjacent styrene repeat unit seems to be confirmed. The proposed mechanism is a McLafferty rearrangement. In addition to this, the hydrogen end group promotes a direct scission mechanism.

When the main chain is deuterated, it is shown that, for a given molecular weight, the number of end group at the surface is lower than for hydrogenated one. This observation is related to the lower surface energy associated to the C−D bonds as compared to the C−H ones.

Acknowledgment. The financial support from the "Fonds National de la Recherche Scientifique (FNRS)-Loterie Nationale" (Belgium) and from the “Région Wallonne” (Belgium) for the acquisition of the ToF-SIMS spectrometer is gratefully acknowledged. This work is sponsored in part by the Belgian Interuniversity Attraction Pole Program (PAI-IUAP P4/10) on “Reduced Dimensionality Systems” and by Bayer AG (Leverkusen, Germany) for another part.

References and Notes

(1) Belu, A. M.; Hunt, M. O., Jr.; DeSimone, J. M.; Linton, R. W. *Macromolecules* **1994**, *27*, 1905.
(2) Muddiman, D. C.; Brockman, A. H.; Proctor, A.; Houalla, M.; Hercules, D. M. *J. Phys. Chem.* **1994**, *98*, 11570.
(3) Delcorte, A.; Bertrand, P. *Surf. Sci.* **1998**, *97*, 412.
(4) Vanden Eynde, X.; Reihs, K.; Bertrand, P. In *Proceedings of the 11th International Conference on Secondary Ion Mass Spectrometry SIMS XI*; Gillen, G., Lareau, R., Bennett, J., Stevie, F., Eds.; J. Wiley & Sons Ed.: New York, 1998; p 571.
(5) Vanden Eynde, X.; Bertrand, P. *Surf. Interface Anal.* **1998**, *26*, 579.
(6) Reihs, K.; Voetz M.; Kruft M.; Wolany D.; Benninghoven, A. *Fresenius J. Anal. Chem.* **1997**, *358*, 93.
(7) Williams P. Ion and Neutral Spectroscopy. In *Practical Surface Analysis*; Briggs, D., Seah, M. P., Eds; John Wiley & Sons: Chichester, U.K., 1992; Vol. II, p 197.
(8) Vanden Eynde, X.; Bertrand, P.; Jérôme, R. *Macromolecules* **1997**, *30*, 6407.
(9) Weng, L. T.; Bertrand, P.; Lauer, W.; Zimmer, R.; Busetti, S. *Surf. Interface Anal.* **1995**, *23*, 879.
(10) Vanden Eynde, X.; Weng, L. T.; Bertrand, P. In *Proceedings of the 10th International Conference on Secondary Ion Mass Spectrometry SIMS X*; Benninghoven, A., Hagenhoff, B., Werner, H. W., Eds.; J. Wiley & Sons Ed.: New York, 1997; p 727.
(11) Vanden Eynde, X.; Fallais, I.; Devaux, J.; Bertrand, P. In *Proceedings of the International Conference on Polymer-Solid Interface*, 2nd ed.; Pireaux, J.-J., Delhalle, J., Rudolf, P., Eds; Presses Universitaires de Namur: Namur, Belgium, 1998; p 473.
(12) Vanden Eynde, X.; Matyjaszewski, K.; Bertrand, P. *Surf. Interface Anal.* **1998**, *26*, 569.
(13) Shard, A. G.; Davies, M. C.; Schacht, E. *Surf. Interface Anal.* **1996**, *24*, 787.
(14) Leeson, A. M.; Alexander, M. R.; Short, R. D.; Briggs, D.; Hearn, M. J. *Surf. Interface Anal.* **1997**, *25*, 261.
(15) Hittle, L. R.; Proctor, A.; Hercules, D. M. *Macromolecules* **1995**, *28*, 6238.
(16) Hittle, L. R.; Proctor, A.; Hercules, D. M. *Anal. Chem.* **1994**, *66*, 108.
(17) Chilkoti, A.; Castner, D. G.; Ratner, B. D. *Appl. Spectroscopy* **1991**, *45/2*, 209.
(18) Affrossman, S.; Hartshorne, M.; Jérôme, R.; Munro, H.; Pethrick, R. A.; Petitjean, S.; Vilar, M. R. *Macromolecules* **1993**, *26*, 5400.
(19) Affrossman, S.; Hartshorne, M.; Jérôme, R.; Pethrick, R. A.; Petitjean, S.; Vilar, M. R. *Macromolecules* **1993**, *26*, 6251.
(20) Ramsden, W. D. *Surf. Interface Anal.* **1991**, *17*, 793.
(21) Brinkhuis, R. H. G.; van Ooij, W. J.*Surf. Interface Anal.* **1988**, *11*, 214.
(22) Brant, P.; Karim, A.; Douglas, J. F.; Bates, F. S. *Macromolecules* **1996**, *29*, 5628.
(23) Whitlow, S. J.; Wool, R. P. *Macromolecules* **1989**, *22*, 2648.
(24) Strzhemechny, Y. M.; Schwarz, S. A.; Schachter, J.; Rafailovich, M. H.; Sokolov, J. *J. Vac. Sci. Technol.* **1997**, *A15*, 894.
(25) Agrawal, G.; Wool, R. P.; Dozier, W. D.; Felcher, G. P.; Zhou, J.; Pispas, S.; Mays, J. W.; Russell, T. P. *J. Polym. Sci., Polym. Phys.* **1996**, *B34*, 2919.
(26) van der Wel, H.; Baken, J. M. E.; Willard, N. P. In *Proceedings of the 8th International Conference on Secondary Ion Mass Spectrometry SIMS VIII*; Benninghoven, A., Janssen, K. T. F., Tümpner, J., Werner, H. W., Eds.; J. Wiley & Sons Ed.: New York, 1992; p 799.
(27) Occhiello, E.; Morra, M.; Garbassi, F.; Johnson, D.; Humphrey, P. *Appl. Surf. Sci.* **1991**, *47*, 235.
(28) Vanden Eynde, X.; Bertrand, P. *Surf. Interface Anal.* **1997**, *25*, 878.
(29) Painter, P. C.; Coleman, M. M. In *Fundamentals of Polymer Sciences*; Technomic Publishing: Lancaster, PA, 1994.
(30) Young, R. N.; Quirk, R. P.; Fetters, L. J. *Adv. Polym. Sci.* **1984**, *56*, 1.
(31) Bertrand, P.; Weng, L. T. In *Surface Characterization: A Practical Approach*; Scandinavian Scientific Press and VCH Publishers: Weinhem, Germany, 1997.
(32) Weng, L. T.; Bertrand, P. *Mikrochemica Acta* **1996**, *Suppl. 13*, 167.
(33) Schueler, B. W. *Microsc. Microanal. Microstruct.* **1992**, *3*, 119.
(34) Delcorte, A.; Segda, B. G.; Bertrand, P. *Surf. Sci.* **1997**, *381*, 18; Delcorte, A.; Segda, B. G.; Bertrand, P. *Surf. Sci.* **1997**, *389*, 393.

(35) Newman, J. G.; Carlson, B. A.; Michael, R. S.; Moulder, J. F.; Holt, T. H. *Static SIMS Handbook of Polymer Analysis* Perkin-Elmer Corporation Edition: Eden Prairie, MN, 1991.
(36) Briggs, D.; Brown, A.; Vickerman, J. C. In *Handbook of Static Secondary Ion Mass Spectrometry (SIMS)*; John Wiley & Sons: New York, 1989.
(37) Vickerman, J. C.; Leggett, G. J.; Hagenhoff, B.; Briggs, D.; Chilkoti, A.; Bryan, S. R.; McKeown, P. J. *Wiley Static SIMS Library*; John Wiley & Sons Eds.: New York, 1996.
(38) Bates, F. S.; Wignall, G. D. *Phys. Rev. Lett.* **1989**, *57/12*, 1429.
(39) Elman, J. F.; Johs, B. D.; Long, T. E.; Koberstein, J. T. *Macromolecules* **1994**, *27*, 5341.
(40) Hopkinson, I.; Kiff, F. T.; Richards, R. W.; Affrossman, S.; Hartshorne, M.; Pethrick, R. A.; Munro, H.; Webster, J. R. P. *Macromolecules* **1995**, *28*, 627.
(41) McLafferty, F. W.; Turecek, F. In *Interpretation of Mass Spectra*, 4th ed.; University Science Books: Mill Valley, CA, 1993.
(42) Spool, A. M.; Kasai, P. H. *Macromolecules* **1996**, *29*, 1691.
(43) Kingston, E. E.; Eichholzer, J. V.; Lydon, P.; MacLeod, J. K.; Summons, R. E. *Organic Mass Spectrometry* **1988**, *23*, 42.
(44) Apeloig, Y.; Franke, W.; Rappoport, Z.; Schwarz, H.; Stahl, D. *J. Am. Chem. Soc.* **1981**, *103*, 2770.
(45) Leggett, G. J.; Vickerman, J. C. *Int. J. Mass Spectrosc. Ion Processes* **1992**, *122*, 281.
(46) Leggett, G.; Vickerman, J. C.; Briggs, D.; Hearn, M. J. *J. Chem Soc. Faraday Trans.* **1992**, *88*, 297.
(47) Huan, C. H. A.; Wee, A. T. S.; Gopalakrishnan, R.; Tan, K. L.; Kang, E. T.; Neoh, K. G.; Liaw, D. J. *Synth. Met.* **1993**, *53*, 193.
(48) Chiarelli, M. P.; Proctor, A.; Bletsos, I. V.; Hercules, D. M.; Feld, H.; Leute, A.; Benninghoven, A. *Macromolecules* **1992**, *25*, 6970.

MA981558I